IMPROVED GEOMETRY OF INTEGRATED MAGNETICS FOR THE HYBRIDGE TOPOLOGY

Søren Petersen

Alcatel Space Denmark
Lautrupvang 2, DK-2750 Ballerup, Denmark
E-mail: soren.petersen@alcatel.dk

ABSTRACT/RESUME

A new geometry of integrated magnetics [1] for the Hybridge topology [2] is presented. The geometry is designed for the low voltage and high current required by modern digital applications.

The new integrated magnetics makes it possible to build high-efficiency low-cost DC/DC converters, because it features low stray inductance and eliminates the need for coil formers, ground air gaps and interleaving of the primary and secondary windings.

Experimental results obtained for a 50V to 3.3V 25A DC/DC converter with galvanic isolation, demonstrates efficiency above 91% for half to full load current.

1. CIRCUIT TOPOLOGY

The Hybridge topology [3], also known as the current doubler topology, is well suited for low-voltage high-current applications because the amplitude of the secondary and inductor current is approximately half the load current and the voltage lost by rectification is only one diode drop.

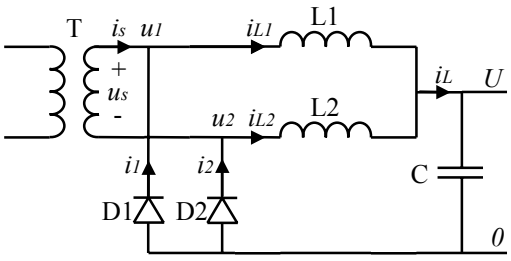

Fig. 1 The Hybridge Topology

The function of the circuitry is shown by the waveforms in fig. 2. The primary voltage can be generated by a full-bridge, a half-bridge or a push-pull topology. The average value of u_1 and u_2 is equal to the output voltage U. The secondary current (i_S) is identical to i_{L1} for $0 \le t < DT$ and to $-i_{L2}$ for $T/2 \le t < T/2+DT$.

Note that the ripple current of the two inductors (i_{L1}, i_{L2}) tend to cancel each other when added together (i_L).

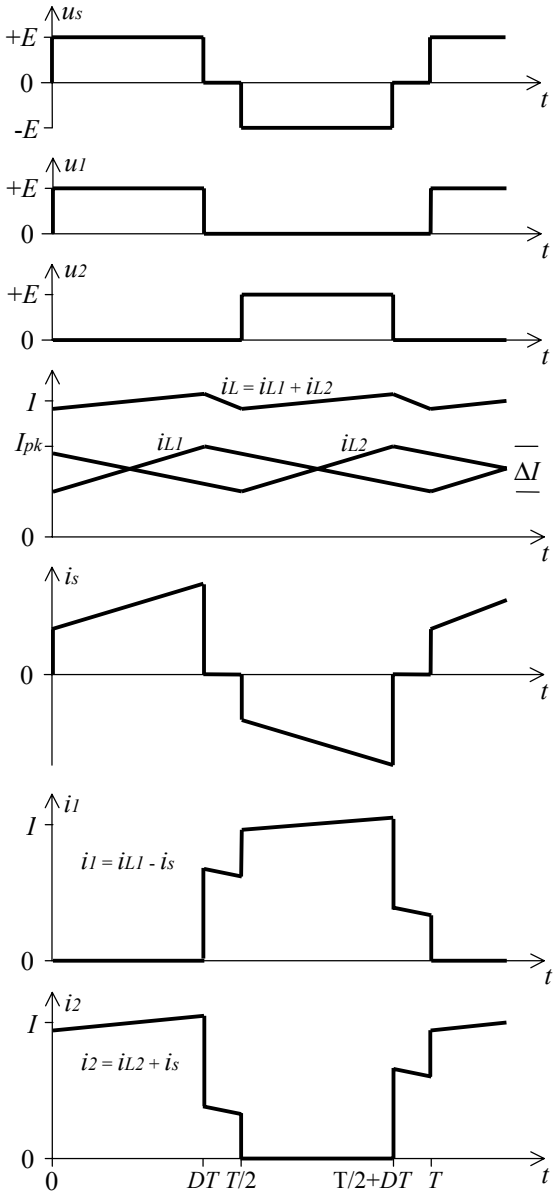

Fig. 2 Schematic waveforms for the Hybridge

As described in [3], the transformer and the two chokes can be integrated on a single core with three legs and air gaps in the side legs. This core could be made of two E-cores as shown in fig. 3. The transformer is wound on the centre leg and the chokes are wound on the two side legs.

1.1 Design Considerations

The number of turns (N) in the inductor- and the secondary windings of the integrated magnetics have to be equal, in order to maintain the flux balance between the three legs of the core. The minimum number of turns needed to avoid saturation of a core whilst at the same time keeping the inductor ripple current to an acceptable level, is calculated in this section.

Assuming an equal cross-sectional area of all three core legs, the maximum flux density (B_{pk}) occurs in the inductor legs. Therefore, the required number of turns is determined by the inductor design. The inductors on the integrated magnetics can be designed in the same way as normal inductors.

According to Ampere's law, eq. 1, the magnetic field (H) in the air gap of the inductors (δ) is given by eq. 2, assuming infinite permeability of the core material.

$$\oint \mathbf{H} \cdot d\mathbf{s} = N \cdot I \tag{1}$$

$$H \cdot \delta = N \cdot I \tag{2}$$

The flux density in the air gap and the core, ignoring fringing flux, is

$$B = \mu_0 \cdot H \tag{3}$$

Eliminating H from eq. 2 and 3 gives

$$B = \frac{\mu_0}{\delta} \cdot N \cdot I \tag{4}$$

Eq. 4 shows that the flux density is proportional to the inductor current and therefore, the flux density waveform is identical to the inductor current waveform. This is also a good approximation for a real inductor with a non-ideal core, if the major part of the energy is stored in the air gap and saturation is avoided.

This means that the maximum allowed flux density ripple (ΔB) is given by the maximum peak flux density for the core material (B_{pk}) and the ratio of allowed peak-to-peak ripple current (ΔI) to the peak current (I_{pk}).

$$\Delta B = B_{pk} \cdot \frac{\Delta I}{I_{pk}} \tag{5}$$

On the other hand, the flux density ripple that will result from applying the actual inductor voltage, can be found using Faraday's law, eq. 6.

$$U = -N \cdot \frac{d\Phi}{dt} \tag{6}$$

Fig. 2 shows that u_1 is constantly equal to zero in the period DT < t < T and therefore the inductor voltage is equal the output voltage. The flux ripple ($\Delta\Phi$) is found by integration of eq. 6.

$$\Delta\Phi = \frac{1}{N} \int_{DT}^{T} U_{out} \cdot dt \tag{7}$$

$$\Delta\Phi = \frac{U_{out} \cdot (1-D) \cdot T}{N} \tag{8}$$

Assuming an equal cross sectional area (A) of core and air gap, the flux density ripple is

$$\Delta B = \frac{\Delta\Phi}{A} \tag{9}$$

and from eq. 8

$$\Delta B = \frac{U_{out} \cdot (1-D) \cdot T}{N \cdot A} \tag{10}$$

The flux density ripple given by eq. 10 shall be less than or equal to the allowed value given by eq. 5.

$$\frac{U_{out} \cdot (1-D) \cdot T}{N \cdot A} \leq \frac{\Delta I}{I_{pk}} \cdot B_{pk} \qquad (11)$$

The required number of turns is found from eq. 11.

$$N \geq \frac{U_{out} \cdot (1-D) \cdot T}{A \cdot B_{pk}} \cdot \frac{I_{pk}}{\Delta I} \qquad (12)$$

In the following the ratio $I_{pk}/\Delta I$ is called the ripple factor (K_r). Choosing the ripple factor is a trade-off between power loss in the integrated magnetics and power loss in the power transistors. High ripple current causes increased power loss in the transistors and low ripple current requires a high number of inductor turns, which results in high conduction losses in the integrated magnetics. Experience has shown that a good trade-off is a ripple factor of two.

2. DERIVING THE NEW GEOMETRY

The conventional core for the integrated magnetics is shown in fig. 3. The cross section of the legs is close to square in order to minimise the mean length of turns for a given cross section area. The window area for each winding is close to the cross section area of the core legs.

The core shown in scale on fig. 3 is suitable for a 3.3V 25A converter (A is 44mm²). According to eq. 12, and assuming typical values of D, T, B_{pk} and K_r like those used in section 5, at least three turns is required for the secondary and inductor windings.

The low number of turns and the high conductor cross sectional area needed to carry the large output current means that foil windings are preferred. Using foil windings represents a practical problem because the terminals have to break out of the coil former at a right angle to the winding direction and the width of the terminals must be several times less than the width of the windings.

In order to utilise the height of the winding window without problems due to skin and proximity effect, the primary and secondary windings have to be interleaved by splitting the primary winding in two parts and placing the secondary between these.

Both of these practical difficulties can be avoided if the number of turns can be reduced to one. Using only one layer instead of three in the secondary winding, eliminates the need for interleaving layers. The single turn secondary, not enclosed by the primary, and the inductor windings, can break out of the coil at full width without the need for rectangular bending.

The ideal core shape for one turn windings is derived form the following considerations.

1) Eq. 12 shows that the number of turns can be reduced from three to one by increasing the cross section area of the core legs by a factor of three.

2) No interleaving of winding means that only a low profile winding window area is needed.

3) The balance between core material and conductor material means that the legs of the core have to be thin.

The core geometry that satisfies these requirements, realised by two E-cores, is shown in scale in fig. 4.

The same core geometry can also be realised by three stacked I-cores, as shown in fig. 5. I-cores have several advantages over E-cores as described in section 3.

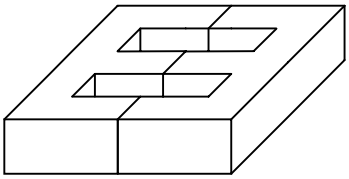

Fig. 3 Conventional core geometry with quadratic cross section of the three legs

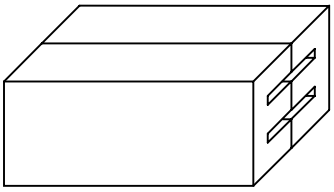

Fig. 4 New core geometry designed for one-turn secondary- and inductor windings

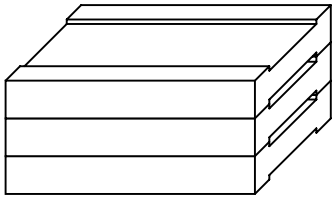

Fig. 5 New core geometry realised by I-cores

3. PROPERTIES OF THE NEW GEOMETRY

A prototype of the new core is shown in fig. 6. The windings are wound directly on ferrite I-cores which are stacked with thin sheets of an electrical isolating material in between. The stack is kept together with a pair of brackets, separated from the cores by sheets of thermally conductive rubber.

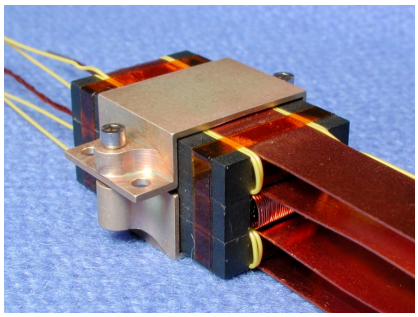

Fig. 6 Prototype of the new integrated magnetics made for a 3.3V 25A converter

Note that the foil windings leave this compacted unit in a very straightforward manner and that efficient cooling is possible via the brackets.

The connections of the foil windings are shown on fig. 7. The rectifiers are connected through short, wide and parallel conductors. Therefore the stray inductance of the loop consisting of the secondary winding and the two rectifiers is very low. This is essential when switching high load currents. Also the skin effect is minimised by this layout.

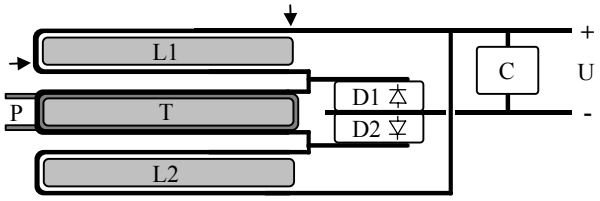

Fig. 7 Schematic cross section of an I-core integrated magnetics connected to rectifiers and output capacitor.

Air gaps for the inductors have to be ground into the side legs if E-cores are used. However, using I-cores, the grinding process is eliminated because the air gaps are obtained by separating the I-cores by sheets of isolating material with well-defined thickness.

Furthermore, due to tolerances of the grinding process, a small air gap in the centre leg of the E-core construction can not be avoided. This air gap makes the integrated magnetics less ideal since it increases the reluctance of the centre leg. This is not a problem with the I-core construction since no additional gap will occur.

Coil formers are not required for the I-core construction because it consists of one I-core for each coil. The coils can be wound directly on the cores, separated just by a layer of tape. This in combination with the simple shape of the I-cores, minimises the design time as well as the production cost of the integrated magnetics.

As the air gaps of the I-core geometry not are enclosed by the inductor windings, increased fringing flux could be expected. However, according to eq. 4 the gap length is proportional to the number of turns. Therefore reducing the number of turns reduces the gap length. Furthermore, the gap length is reduced by a factor of two, because each of the gaps in the E-core unit is replaced by two gaps in the I-core unit. Reducing the gap length also reduces the fringing fields from the gaps.

In general a large fringing field will be radiated from an inductor wound on the centre leg of an E-core with air gaps in the side legs, but this is not the case for the integrated magnetics. The voltage applied to the series connection of the inductors on the side legs is equal the voltage on the secondary winding and thus the sum of the flux generated by the two inductors is equal the flux generated by the secondary winding. Therefore, the flux generated by the transformer on the centre leg will be guided through the side legs by the inductors.

In praxis, the fringing flux has not caused any problems.

A drawback of the new geometry is the reduced ability for choosing optimum turns-ratio. As the number of turns is reduced, the step between possible turns-ratios is increased accordingly. This means the for some low input voltage applications it is not possible to obtain the duty cycle that gives the best efficiency.

4. ELIMINATING THE SECONDARY WINDING

Faraday's law gives the change of flux through the core for L1. This flux flows mainly through the core in T. A minor part flows through the core in L2 and another minor part through the exterior as fringing flux.

Due to this distribution of the flux, the voltage over the inductor L1 is not equally distributed along the inductor winding. The voltage across the part between the two arrows in fig. 7 is close to zero, because it is

outside the core. If for instance an oscilloscope is connected, only some fringing flux will pass through the loop formed by the two wires and the part of the inductor. The full inductor voltage can be measured across the part inside the core because all the flux through L1 passes the loop. The same applies for L2.

A similar consideration shows that the secondary voltage is not equally distributed along the secondary winding either. Measuring across the part between the cores for L1 and T, the flux through the measuring loop is equal to the flux through L1 and therefore, the voltage over this part is equal the inductor voltage. For the same reason, the voltage over the remaining part of the secondary winding, is equal the voltage across L2.

As the inductor L1 and the secondary are connected at D1 and the voltage over the two is equal inside the core they can be replaced by a single conductor, without altering the function of the integrated magnetics, see fig. 8.

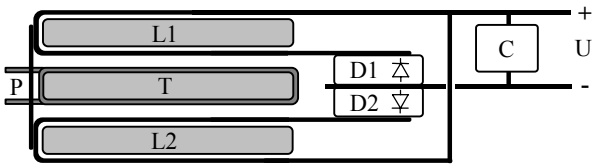

Fig. 8 Schematic cross section of the I-core integrated magnetics with eliminated secondary winding.

The secondary current is a pure AC-current and if the ripple current in the inductors is ignored for a while, the choke current becomes a pure DC-current. Because these two currents are non-correlated, the sum of the two currents will cause the same power loss in a resistor as the sum of the power losses each of the currents will cause in the same resistor.

Assuming equal resistance of the two internal conductors, they can be replaced by one of the two, without increasing the total power loss. This is also the case for the two conductors between the cores for T and L2. For this reason, the secondary winding can be eliminated without increasing the power loss of the integrated magnetics, resulting in a smaller and cheaper unit.

When the conductors are merged, i_{L1}, i_{L2} and i_s no longer exist but are replaced by i_1 and i_2, see fig. 2. If the ripple current is not ignored as above, the RMS value of all currents will be larger, but i_1 and i_2 will be less affected because the ripple current of the inductors and secondary tend to phase out each other. Therefore, the power loss with merged conductors will be reduced.

5. EXPERIMENTAL RESULTS

The new geometry of the integrated magnetics, is tested on an elegant breadboard of a DC/DC converter that converts an input voltage of 47–53V to 3.3V 0–25A. The following operation conditions are chosen:

Number of turns (N):	1
Switching frequency ($1/T$):	120kHz
Maximum flux density (B_{pk}):	300mT
Duty cycle (D):	0.40
Ripple factor (K_r):	2

5.1 Calculating the dimensions of the I-core

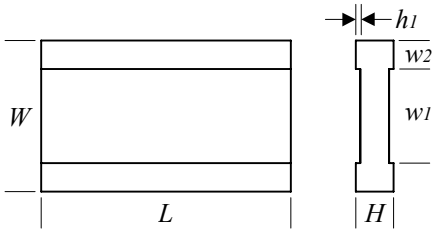

Fig. 9 Dimensions of the I-core

The overall height of the integrated magnetics is chosen to match the building height of the other components of the converter. The height of one I-core (H) is therefore chosen to be 5mm.

Based on the skin depth of approximately 0.2mm, the conductor thickness is chosen to be 0.3mm. This requires a height of 0.6mm to allow for isolation material and tolerances. As the secondary winding can be left out for the one-winding solution, only a window height (h_1) of 0.6mm is required on each side of each I-core.

This leaves a material thickness of $H - 2h_1 = 3.8mm$ for conducting the magnetic flux. The width of the contact area between stacked I-cores (w_2) has to be equal to this thickness in order not to form a bottleneck for the flux.

The necessary conductor width for conducting the output current is approximately 10mm. In order to leave some space for auxiliary windings and tolerances, the window width (w_1) is chosen to 12.4 mm. The width of the core therefore becomes $w_1 + 2(H - 2h_1) = 20.0mm$.

The cross section area of the core is found by eq. 12.

$$A = \frac{3.3V \cdot 1.1 \cdot (1 - 0.4)}{300mT \cdot 120kHz} \cdot 2 = 121mm^2$$

The output voltage is multiplied by 1.1 to account for the voltage drop in semiconductors.

The required length of the I-cores (L) is therefore $A/(H-2h_1)=31.8mm$. The chosen length is 33mm to allow for some tolerances. These I-cores stacked to a core for an integrated magnetic are shown 1:1 in fig. 5.

5.2 Breadboard

The elegant breadboard is built using space quality parts or equivalent. It consists of an input filter (upper left), full-bridge with 100V radiation hardened MOSFET's (lower left), integrated magnetics (lower middle), synchronous rectification with two 30V radiation hardened MOSFET's in SMD2 housing (lower right), bipolar PWM controller (upper right) and a fly-back converter for internal supply (upper middle). Special attention has been paid to obtain low stray-inductance in series with the rectifiers.

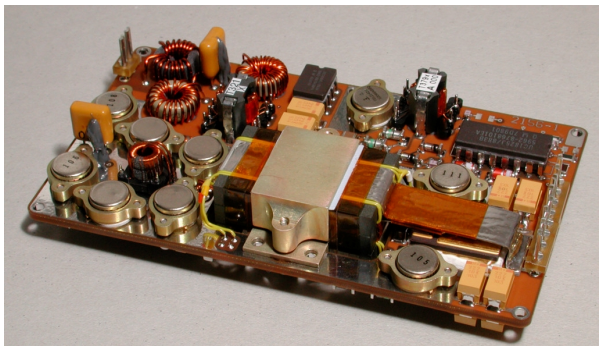

Fig. 10 Elegant breadboard of the 3.3V 25A converter. Size: 60 mm x 105 mm. Mass: 140 g.

5.3 Test Results

The stray-inductance in series with the rectifiers is measured to 14nH, including the leakage inductance of the transformer.

The primary voltage, primary current and the voltage across one of the rectifiers are measured with a 200Mhz oscilloscope at full load current, see fig. 11. The primary current should look like the secondary current (i_S), shown in fig. 2 but deviates in the intervals where the primary voltage is zero. This is caused by use of synchronous rectification and a clamped bridge.

The efficiency of the breadboard is measured with respect to load current and base-plate temperature, see fig. 12. The power consumption with no load is 2.6W at 22°C. Note that the breadboard includes an auxiliary converter for internal supply as well as filtering.

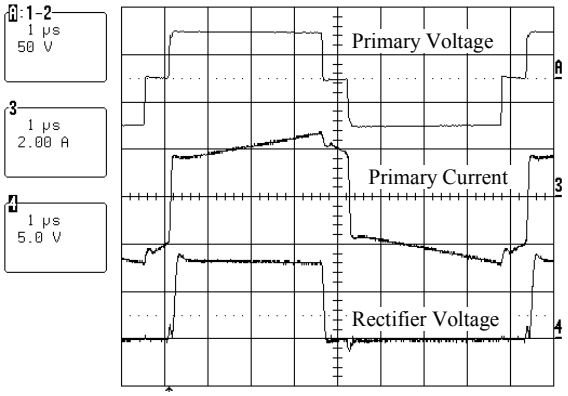

Fig. 11 Measured waveforms at full load current.

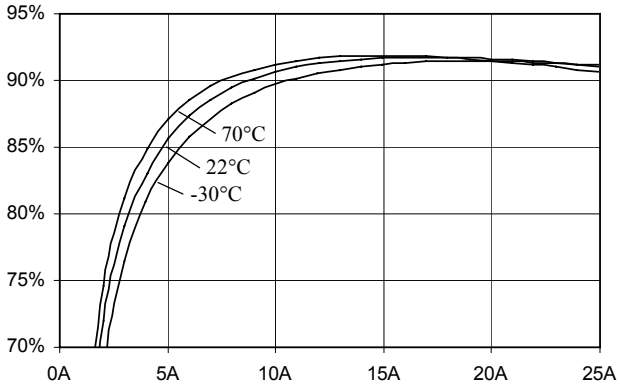

Fig. 12 Measured efficiency.

6. CONCLUSION

The theory for deriving a new geometry of integrated magnetics for the Hybridge topology is presented and verified by test results.

The results obtained for a 50V to 3.3V 25A DC/DC converter, with galvanic isolation, demonstrate high efficiency over a broad load current range, and clean waveforms indicating low stress of components.

Based on excellent performance and ease of manufacturing, the new integrated magnetics will be developed for production of space flight quality units.

7. REFERENCES

1. US Patent no. 5,335,163, EU Patent no. 0 5557 378.

2. US Patent no. 4,899,271.

3. Peng C., Hannigan M. and Seiersen O., *A New Efficient High Frequency Rectifier Circuit,* HFPC, June 1991 Proceedings.